Developing a Universal Framework for Modeling DC-Connected Hybrid Real and Virtual Energy Storage Systems

Derek Jackson , Member, IEEE, and Yue Cao , Senior Member, IEEE

Abstract—A universal modeling framework for hybrid energy storage systems is proposed. The framework can model various energy storage types, both real and virtual. Hybrid systems employ power electronics connected in various topologies to coordinate the operation of multiple storages, which this framework generalizes into a single, switching-averaged model. Multiple common dc/dc converter types are shown to be compatible with this framework. The universal model aims to simplify system design and analysis by recognizing the commonalities of hybrid topologies, converter operation, and storage dynamics to focus on the overall system behavior and energy bandwidth requirements. The generalized parameters can be transformed into real values to continue the system design process. This paper focuses on defining the theory of the universal model. A demonstration of the model shows the framework's validity by comparing simulation results to the proven physics switching models.

Index Terms—Hybrid energy storage systems, virtual energy storage, mathematical modeling, battery, supercapacitor, thermal storage, HVAC, power electronics.

I. INTRODUCTION

HE complex loads of modern power systems include a wide variety of load dynamics that span multiple timescales. Hybrid energy storage systems (HESS) are employed to accommodate these characteristics by utilizing multiple energy storage types. There are many storage solutions developed spanning various physics domains (e.g., electrochemical, thermal, mechanical), each with their own pros and cons that can be combined within a hybrid system to achieve optimal performance. A relatively recent solution called virtual energy storage (VES) has gained attention, which aggregates controllable unidirectional loads inherent to the system. These loads have inertia or energy capacity and can effectively act as bidirectional storage by modulating the power consumption dynamically using power

Received 3 February 2024; revised 26 July 2024 and 5 September 2024; accepted 3 October 2024. Date of publication 23 October 2024; date of current version 23 May 2025. This work was supported by the U.S. National Science Foundation (NSF) under Award 2146350. Article no. TEC-00125-2024. An earlier version of this paper was presented in an oral session at the 2023 IEEE Energy Conversion Congress & Expo (ECCE), Nashville, Tennessee, USA [DOI: 10.1109/ECCE53617.2023.10362895]. (Corresponding author: Yue Cao.)

The authors are with the School of Electrical Engineering and Computer Science, Oregon State University, Corvallis, OR 97331 USA (e-mail: jacks-der@oregonstate.edu; yue.cao@oregonstate.edu).

Color versions of one or more figures in this article are available at https://doi.org/10.1109/TEC.2024.3484310.

Digital Object Identifier 10.1109/TEC.2024.3484310

electronics. Examples of VES include a building's heating, ventilation, and air conditioning (HVAC) system [2], [3], or a hot water tank heater [4]. VES is an excellent solution for HESS, as the hardware is already part of the system.

While hybrid storage has many appealing traits, it is a complex system that involves many design decisions spanning storage selections, power electronic converter and system architectures, and control strategies. Design and analysis can become overcomplicated or intractable when all of these decisions are considered. The numerous approaches to energy storage modeling further convolute the processes. Hence this work aims to simplify the design and analysis of dc-connected hybrid energy storage systems through a universal framework for modeling. A similar framework may be developed for ac-connected systems, but is left for future work. The framework is divided into two sections: one focuses on a universal model for any energy storage device, and the second is a generalized model for a wide variety of HESS with connected power electronics.

A. Energy Storage Modeling

For electrical engineering design and analysis, electrical equivalent circuit modeling is a popular approach for energy storage system design. This allows electrical engineers to evaluate the feasibility of various storage options, including system stability, power efficiency, and sizing/cost. However, the wide variety of available energy storage equivalent circuit models make direct comparisons and trade-off studies challenging, especially when involving multiple storage types within an application. The distinction between circuit components that affect power dynamics and energy storage capabilities can also be unintuitive.

Multiple circuit modeling approaches exist across different energy storage physics. For example, electrochemical batteries can be modeled with a simple Thevenin voltage source and internal resistance, or use a more detailed RC-parallel impedance, or utilize lesser-known circuit elements such as the Warburg or constant-phase element (CPE) [5], [6], [7], [8], [9], [10], [11], [12]. Another example are supercapacitors, where a number of different circuit networks are considered for modeling the internal impedance and charge distribution, including RC-branches, RC-ladders, transmission line models, and sometimes include voltage-dependent variable impedances [13], [14], [15], [16], [17], [18]. The internal impedance circuit network for the storage

0885-8969 © 2024 IEEE. Personal use is permitted, but republication/redistribution requires IEEE permission. See https://www.ieee.org/publications/rights/index.html for more information.

model typically reflects the level of fidelity desired in the analysis. Each series or parallel-connected RC-branch or RC-ladder can represent a storage's dynamics for a specific timescale. Additionally, more complex networks could capture more detail of the intricacies within a device. A good example of this is for hydrogen fuel cells. In [19], the fuel cell is simply modeled with a voltage source and resistance, while [20] proposes an intricate circuit model to capture the internal mechanisms of fuel cell operation. Another proposed model defines two different equivalent circuits, depending on the fuel cell's output power [21].

To summarize, existing energy storage electrical equivalent circuit models often include Thevenin equivalents with a dependent open-circuit voltage and a series of impedance networks to track responses to transient loads. There are a handful of other energy storage physics such as flywheel, pumped hydro, and thermal that are less commonly modeled as an equivalent circuit [22], [23], [24], [25], [26]. However, their interaction with an electrical system as a mechanism of energy storage can be represented by an equivalent circuit. Some effort in modeling these type of energy storage physics with a unified equivalent circuit can be found in [27], [28] but is limited in its ability to model the interface between the storage physics and an electrical circuit through power electronics. For VES, models are either high-level that abstract away many of the dynamics and losses of the system [3], [29] or use switching circuit models [2], which are costly to simulate or offer little value for long-term system-level design. Existing literature lacks an attempt to formulate the VES in the same model framework as real storage.

This paper defines an equivalent-circuit-based universal energy storage model (UESM) capable of accurately modeling many storage devices, both real and virtual. The UESM identifies the standard methods to represent time constants and dynamics and defines a generalized template that applies to any energy storage device. This universal representation simplifies design studies and comparisons in addition to model development with this single energy storage model template and allows different storage physics to be more directly compared to each other. To present a simple generalized energy storage model, not all equivalent circuit models in the literature fit within the UESM framework. Instead, common topologies among models are identified and used within the UESM. It is important to note that this universal framework does not aim to replace all existing equivalent circuit models. Rather, this framework is developed for system integration and analysis, where other complex or device specific circuit networks will be more applicable for different design stages.

B. Hybrid Energy Storage System Modeling

Simply connecting different energy storage types in parallel is not sufficient for a HESS. Different storage types operate at varying voltage levels, which can also vary significantly throughout their operation, preventing their direct connection. Thus, power electronics are a critical middle-man to connect within a HESS. Power electronics also enable the control of resource sharing and voltage and power regulation that are needed to achieve optimal operation objectives [30], [31], [32], [33], [34], [35], [36].

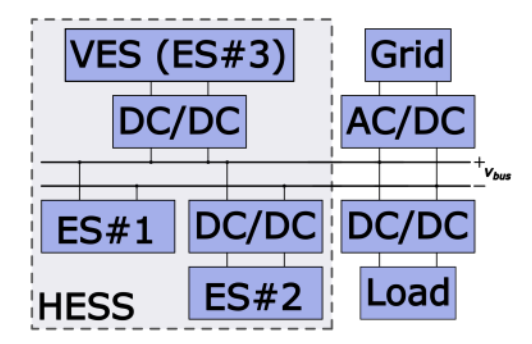


Fig. 1. A high-level diagram of an example dc-connected hybrid energy storage system with a main grid connection and generic load.

Using power electronics, a variety of topologies exist to integrate multiple storage types into a HESS. The topologies can be classified into active, semi-active, and passive configurations [37], [38]. Selecting which configuration is optimal for an application is not straightforward and requires detailed analysis to determine their performance and cost, among other factors. Conventionally, a topological change in a system requires developing a separate model for simulation studies. However, there is little variation in system dynamics among the different configurations when considering the core behavior of a HESS. Since the primary objective of a hybrid system is the controlled coordination between multiple storage types, understanding each of their capabilities along with their required hardware is the focus of analysis. Specific converter types and system architectures are merely a means to achieve the power sharing coordination. Thus, a simplified representation of the converters can be made as a part of a HESS.

C. Paper Overview and Contributions

This paper presents a universal hybrid energy storage model (UHESM) that incorporates a wide variety of dc/dc converter-based architectures. An example of such a hybrid system is provided as a high-level diagram in Fig. 1. Instead of starting with a predetermined storage selection and architecture, the UHESM can be used to explore possible solutions by identifying system specifications that narrow down and guide the design process. In addition to its generality, it models the dynamics of a HESS with sufficient fidelity for a large variety of analysis. This paper does not implement every type of energy storage physics and converter type in this framework, as existing storage types and converter topologies are numerous. Rather, this work aims to show the feasibility and applicability of the proposed universal framework and provide enough detail for others to implement specific storage types into this modeling framework.

It is entirely possible that the universal framework will need to be updated when more storage types are explored. Without over-complicating the modeling effort, this work shows that a significant number of existing energy storage devices are compatible with such a framework.

The proposed framework is presented in two stages. First, UESM is defined, capable of accurately modeling any energy storage, both real and virtual. This universal representation allows all energy storage mediums to be directly compared to

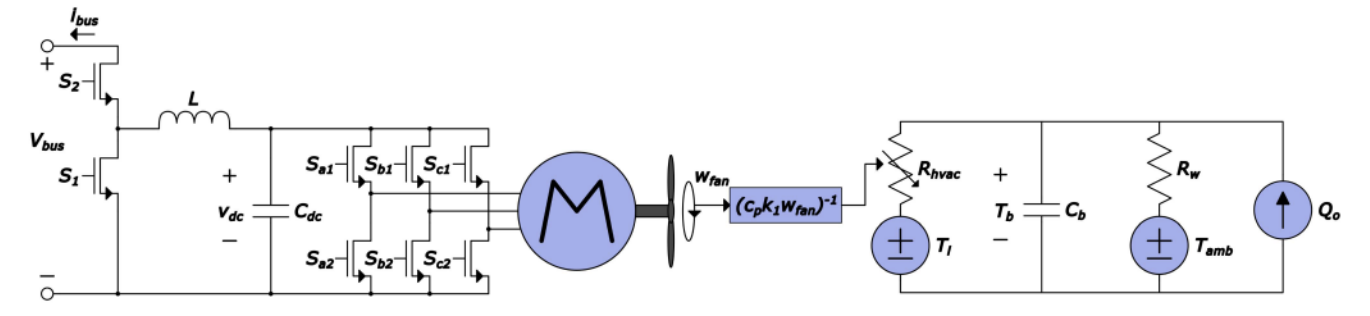


Fig. 2. HVAC-based virtual energy storage in electric circuit representation.

each other, simplifying design studies and comparisons. Second, a universal model for HESS is provided that can represent a wide array of system architectures and power electronic converters. The two stages combined creates the UHESM. The contributions of the UHESM include the following:

- 1) A universal representation for many energy storage types.
- A common modeling theory unifying real and virtual storage.
- A generalization of hybrid energy storage converter types and system topologies.
- A modeling framework that simplifies design exploration and analysis.

Prior to introducing the modeling framework, the virtual energy storage concept is discussed in Section II to provide readers with the necessary background knowledge to understand its compatibility with this work. The UESM is presented in Section III with a few examples of energy storages modeled under this framework provided in Section IV. The UHESM is given in Section V. A demonstration of the UHESM is provided in Section VI, accompanied with a comparison to the switching model simulation and discussion. The paper concludes with a summary and proposed future work in Section VII.

II. VIRTUAL ENERGY STORAGE CONCEPT

The energy buffering behavior in VES is realized by controlling thermal and inertial loads inherent to a system. While these are usually unidirectional loads, they can behave in the same functionality as real energy storage. Neither real nor virtual storage *creates* energy, they only *store* energy for later use. From an average energy usage perspective, temporarily reducing the amount of power an inherent load draws is equivalent to supplying that amount of power. This section will cover how a building's HVAC cooling system can be operated to behave as a VES. The theory, hardware, controls, and modeling details are included to provide the necessary background information to understand the VES concept.

A. HVAC System and Operation

The primary energy storage medium is the thermal capacitance of the air within the building. While in cooling mode, energy is expended to maintain a comfortable temperature. External air temperatures, solar radiation and internal heat

generation sources, such as from humans, electronics, and lighting, counteract this cooling effort. While remaining within a nominal temperature range, the HVAC system can modulate its power consumption to act as a power bandpass filter. The lower frequency limit of the filter ensures temperatures remain within the comfort zone, and the upper frequency limit prevents unwanted acoustic noise and equipment wear caused by the speed adjustment of the HVAC system [2].

A power electronic-based architecture of the HVAC system is shown in Fig. 2. It consists of a dc/dc converter, hex-bridge inverter motor driving a 3-phase permanent magnet synchronous motor (PMSM) connected to the HVAC fan, and the lumped-capacitance thermal equivalent circuit model of the building. HVAC thermal modeling is based on [2], [3] where the mass flow rate \dot{m} of the air is proportional to the fan speed w_{fan} (1), and the power consumption P_{fan} of the motor is proportional to the fan speed cubed (2). The cooling system's heat transfer Q_{hvac} , given in (3), is determined by the temperature difference between the cooling air T_l and building's air T_b and is proportional to the specific heat capacity c_p and \dot{m} .

The lumped thermal model of the building is given in (4) where the change in building temperature is driven by conduction with the outside air temperature T_{amb} through the insulated walls with resistivity R_w , Q_{hvac} , and the combined heat gain Q_o of external and internal heat sources. C_b is the building's thermal capacitance. The thermal circuit in Fig. 2 is equivalent to (4), where Q_{hvac} and the heat transfer with the outside air both behave as a series connected resistor and voltage source. The variable HVAC fan speed results in a variable resistor $R_{hvac} = (c_p \dot{m})^{-1}$. Q_o is not dependent on the building's temperature and is thus modeled as a current source.

$$\dot{m} = k_1 w_{fan} \tag{1}$$

$$P_{fan} = k_2 w_{fan}^3 \tag{2}$$

$$Q_{hvac} = c_p \dot{m} (T_l - T_b) \tag{3}$$

$$C_b \frac{dT_b}{dt} = \frac{1}{R_w} (T_{amb} - T_b) + Q_{hvac} + Q_0 \tag{4}$$

B. HVAC and VES Controls

In this control scheme the dc/dc converter indirectly regulates the building's temperature and performs the power filtering while the hex inverter regulates the dc-link capacitor voltage

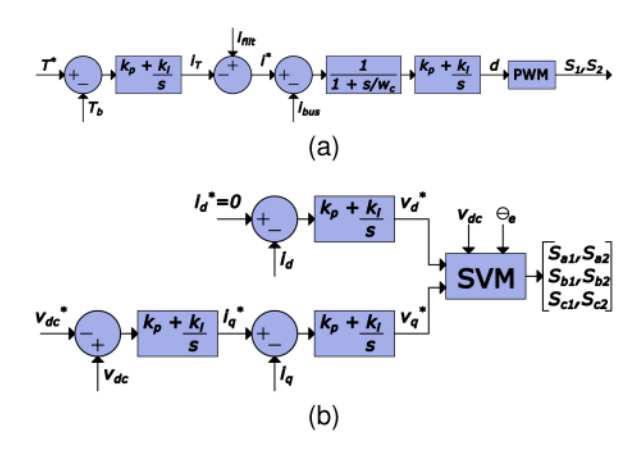


Fig. 3. VES control system where (a) regulates v_{bus} using the dc/dc converter and (b) regulates v_{dc} using the motor drive.

 v_{dc} between the two converters by adjusting the input current of the motor. The roles of the two converters are interchangeable, but this control approach conforms to the UESM framework. By having the motor drive regulate v_{dc} , the system behaves as a power electronic connected energy storage device. Similar to a battery, the dc voltage regulation acts as a series impedance to an "open-circuit" voltage. Section IV-C further discusses this concept. A diagram for the control system is shown in Fig. 3.

The dc/dc converter controller (Fig. 3(a)) consists of a temperature PI regulator cascaded with a current compensator driving the PWM signals duty-cycle d. The converter's output current i_{bus} tracks the difference between temperature regulation current i_{T} and power filtering command current i_{filt} . i_{filt} can be implemented in a couple of different ways. In [2], a power bandpass filter is fed into a 2-D lookup table that calculates the necessary fan speed bias to achieve the power filtering. This approach requires an additional feedback loop for fan speed regulation but effectively behaves the same as Fig. 3(a). In this work, i_{filt} handles a specified bandwidth of the v_{bus} controller output current command. The remaining v_{bus} regulating current is handled by the other storage devices within the HESS. This HESS control scheme is demonstrated in Section VI.

The dc/ac inverter control's (Fig. 3(b)) primary goal is to govern v_{dc} . This is achieved by adjusting i_{sq} , the rotating reference frame's q-axis current. The d-axis current i_{sd} reference is set to zero to prevent PMSM flux weakening. Space vector modulation is used to derive the inverter switching signals to generate the desired motor terminal voltages v_{sd} and v_{sq} .

III. UNIVERSAL ENERGY STORAGE MODEL

The UESM consists of two isolated but coupled circuits: a state of charge (SOC) domain circuit and an electrical domain circuit, both shown in Fig. 4. The domain coupling occurs through the discharge function $f_Q(\cdot)$ and the component-states function $f_s(\cdot)$. $f_Q(\cdot)$ outputs the discharge current i_Q for the SOC domain, and is a function of the ES output current i_{es} in the electrical domain. $f_s(\cdot)$, a function of the storage's inputs and states, outputs the electrical domain and SOC domain circuit element values. The state-dependent impedances allow capacity

and electrical dynamics to change with respect to the storage's states such as SOC or temperature.

The specific equations for the discharge and component-states functions are energy medium dependent and therefore a general solution for them do no exist. Due to the potentially complex relations the functions must represent, this paper uses a mathematically or experimentally derived lookup table for simulations. However, any approach to implementing these functions can be used, given that they do not contain any internal states.

A. SOC Domain

The SOC domain (left side of Fig. 4) represents the primary storage system of the energy storage and defines how effective it is at storing energy for a period of time and how fast it will passively lose charge. The circuit captures charge capacity, charge redistribution, self-discharge, and external inputs from other non-electrical energy domains. It is a normalized circuit such that voltage $v_{\rm soc}$ is equivalent to the SOC (e.g., $v_{\rm soc}=0.5$ when SOC = 50%). The conversion from the original physics domain to the SOC domain is achieved by using (5)–(7), where x_1 is the original domain value associated with a SOC = 100% and x_0 with SOC = 0% (e.g., for a supercapacitor $x_1=2.7V$ and $x_0=0V$). C' is a capacitance, and R' is a resistance of the original domain.

$$SOC = \frac{x - x_0}{x_1 - x_0} \tag{5}$$

$$C = C'|x_1 - x_0| (6)$$

$$R = \frac{R'}{|x_1 - x_0|} \tag{7}$$

The primary storage element is represented as C_{soc} and is often the largest capacitance in the SOC domain. $v_{\rm soc}$ is the voltage across $C_{\rm soc}$. The discharging/charging of the storage is modeled with i_Q , which is dependent on the output current in the electrical domain i_{es} and $f_Q(\cdot)$. Since no storage can indefinitely hold energy, a self-discharge resistor R_p is included. The RCladder networks, consisting of R_n and C_n for $n \in \{1, ..., N\}$, captures the charge redistribution within the storage medium. The UESM is also capable of modeling SOC changes from external inputs. This is less applicable to closed-system storage mediums such as lithium-ion batteries or supercapacitors, but is useful for open-system mediums such as hydrogen fuel cells, flow batteries, and virtual storage. As an example, the hydrogen in fuel cells are refilled via a fluid inlet while it supplies energy through an electrical terminal. External inputs are represented either as a voltage v_{ext} and resistor R_{ext} branch, or a current

The SOC domain can be modeled using the following generalized state-space equations. Any storage medium includes $C_{\rm soc}$ and thus (8) will always be used. In the case that the modeled storage does not include RC-ladders or external inputs, the related terms can be omitted from (8), or simply set $R_{(\cdot)}=\infty$. The dynamics of the charge redistribution is modeled using (9)

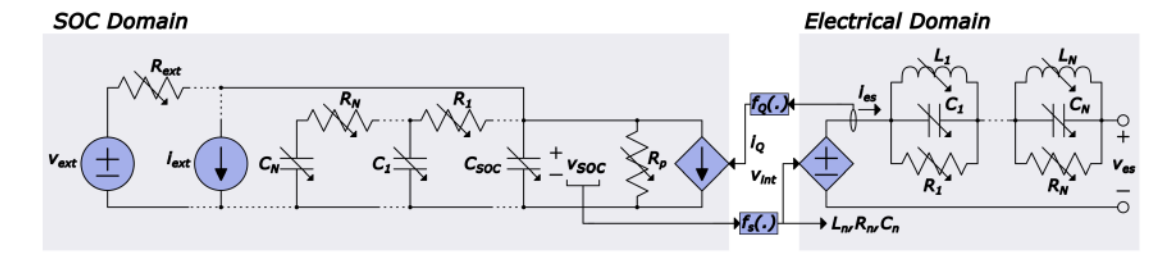


Fig. 4. The universal energy storage model (UESM).

for each RC branch, where $v_{n-1} = v_{\text{soc}}$ for n = 1.

$$C_{\text{soc}} \frac{d}{dt} v_{\text{soc}} = -\left[R_p^{-1} + R_1^{-1} + R_{ext}^{-1} \right] v_{\text{soc}}$$
$$+ R_1^{-1} v_1 - i_Q - i_{ext} + R_{ext}^{-1} v_{ext}$$
(8)

$$C_n \frac{d}{dt} v_n = -\left[R_n^{-1} + R_{n+1}^{-1} \right] v_n + R_n^{-1} v_{n-1} + R_{n+1}^{-1} v_{n+1}$$
(9)

B. Electrical Domain

The electrical domain (right side of Fig. 4) captures the electrical dynamics of the storage. This includes the equivalent internal voltage v_{int} and impedance Z_{es} that facilitates analyses such as response time, transient stability, and the control implementation of the energy system. v_{int} and Z_{es} can either be functions of the system inputs and states or constant, depending on the storage medium and the chosen fidelity. For real storage, the dynamic traits are often inherent to the physics or configuration of the storage medium and limit the energy bandwidth that the ES can supply effectively. For VES, the electrical domain circuit can be customized to an extent but also represents its limitations in supplying power.

The storage's impedance Z_{es} consists of a series connection of a number of RLC-parallel branches $R_n||L_n||C_n$. Each branch captures impedance characteristics on varying time scales, such as seconds, minutes, and hours. These impedance branches are relevant for modeling the charge depletion and recovery effect in batteries [7], or the ion transport effect in supercapacitors [17]. Combined with v_{int} , a single RLC branch can also represent a voltage PID controller [39], [40] and is utilized for VES. Any RLC branch can be reduced to an RC or LR branch by setting $L=\infty$ or C=0.

The electrical domain is modeled using the following generalized state-space equations with inputs v_{int} and i_{es} . An RLC branch's voltage v_n is determined using (10). For $C_n > 0$, v_n is self-defined as it is the state of the n^{th} capacitor. There are two possible state equations for each RLC branch, one for the current through L_n , $i_{L,n}$, and one for the voltage across C_n , v_n . These circuit element states change following (11) and (12), respectively. The storage terminal voltage v_{es} is calculated with (13).

$$v_n = \begin{cases} v_n & , \text{if } C_n > 0\\ (i_{es} - i_{L,n})R_n & , \text{if } L_n < \infty \& C_n = 0\\ i_{es}R_n & , o.w. \end{cases}$$
 (10)

$$L_n \frac{d}{dt} i_{L,n} = v_n \tag{11}$$

$$C_n \frac{d}{dt} v_n = i_{es} - i_{L,n} - v_n R_n^{-1}$$
 (12)

$$v_{es} = v_{int} - \sum_{n=1}^{N} v_n \tag{13}$$

C. Modeling an Energy Storage Device With the UESM

The UESM framework aims to be compatible with many different energy storage devices and physics types. The primary prerequisite for a device's compatibility is that it must be capable of receiving or delivering electrical power. The other prerequisite is that the storage mechanism must be modeled with differential equations, which most physics domains can and are. To create a UESM representation of a storage device, it is also essential to establish how the UESM may be used. The UESM focuses on the storage's electrical interaction with an electrical power system and the storage's primary storage mechanism. It establishes a framework that allows an engineer to understand and model the dynamics that govern how energy is stored, with the SOC domain, and the electrical dynamics involved with transferring energy to and from the primary storage mechanism with the electrical domain.

The two domains of the UESM allow a storage device's energy-storing mechanism to be modeled separately from its electrical interface. This separation is both beneficial and necessary, as the majority of devices store energy within a different physics domain than electricity. The other physics domains often transfer energy through an electrochemical or electromechanical interface, sometimes through complex interactions. The UESM captures this interaction with the discharge function $f_O(\cdot)$.

Representing the conversion between physics domains with a single, stateless function $f_Q(\cdot)$ has limitations. Sometimes, the energy travels through multiple physics domains between the storage mechanism and the electrical interface. For example, the HVAC-based VES receives electrical energy but stores thermal energy through a mechanical interface. A complete system model would consider the rotational inertia of the HVAC motor that stores some quantity of energy. Similarly, the water flowing through the turbine in a pumped-hydro storage system contains some kinetic energy that would not be captured in the UESM. These mechanics are omitted from the UESM to focus on the dynamics of primary concern in hybrid energy storage design for electric power systems.

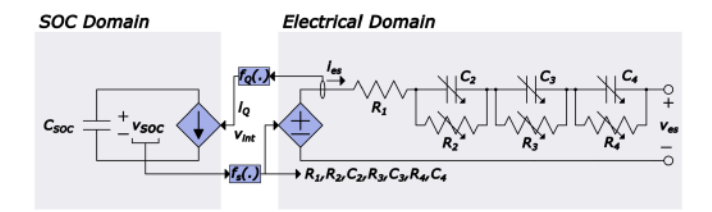


Fig. 5. Battery UESM.

It is assumed that the omitted mechanics of a storage device can be sufficiently approximated as a function dependent on only the SOC and electrical domains of the UESM. This is justified because the energy storage of the mechanics between the SOC domain and electrical domain can largely be ignored in a well-designed hybrid energy storage system. Each storage device has a limited bandwidth to store and supply electrical power. The bandwidth lower limit is related to the storage's energy capacity and ability to retain the energy over time. The bandwidth upper limit corresponds to how quickly the device can deliver or receive electrical energy while satisfying physical constraints. For example, the HVAC-based VES has an upper-frequency limit to avoid unwanted acoustic noise and physical strain on the mechanical component of the system [2]. These constraints limit how quickly the VES can respond to a power command and allow the system's mechanical stage to be well approximated with a steady-state function contained within $f_Q(\cdot)$. So far in developing the framework, the limitation of omitting some mechanics of a storage device does not impede the ability to model the device. However, some minor modeling error is introduced and is explored in Section VI-C.

IV. ENERGY STORAGE REPRESENTATIONS USING THE UESM

This section presents a few UESM representations of popular energy storage devices. It does not comprehensively cover all existing energy storage physics, but serves as a demonstration of the flexibility of the UESM framework.

A. UESM: Lithium-Ion Battery

Representing a lithium-ion battery using the UESM is the most straightforward as it requires minimal adjustments to existing dynamic models in literature, such as [5], [7], [10]. It is common to represent the dynamics of a lithium-ion battery using several series connected RC parallel branches. This series impedance captures the change in resistance from the charge depletion and recovery effects [7]. The electrical domain of the UESM models the same dynamics. In fact, there is little difference between the UESM battery model shown in Fig. 5, and the model presented in [5]. Each RC branch's resistance and capacitance are both a function of the SOC. The open-circuit voltage source is also a function of the SOC, being a linear relation in simple models and a nonlinear relation in more detailed models. The voltage source and RC branch parameters are calculated in the component-states function of the UESM, a function of SOC and discharge current i_Q . Note that the UESM component-states function generally does not depend on i_Q . For

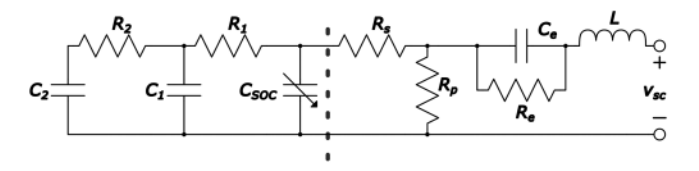


Fig. 6. Supercapacitor model from [17].

this battery model, the electrical domain impedance changes whether the battery is charging or discharging. The sign of i_Q is used instead of the derivative of SOC to help with simulation.

The SOC domain is also similar to existing battery models [5], [7], where a battery's capacity is commonly defined as stored charge in units of amp-hours (Ah). The SOC is thus a ratio between the maximum charge and the charge stored in the battery. Or equivalently, the integration of discharge current $\int i_Q dt$. Given the direct relation between discharge current and SOC, the SOC domain model is simply a single capacitor in parallel with a current source, as shown in Fig. 5. This is also the approach used in [5]. The SOC capacitance is defined as the charge capacity in Coulombs (i.e., $C_{\text{soc}} = Ah \cdot 3600$). The voltage across C_{soc} is equivalent to the battery's SOC, as with all implementations of the UESM. In both [5], and the UESM, the SOC domain current source i_Q is equivalent to the ES output current i_{es} . Some battery models also capture the self-discharge rate, which can be modeled as a resistor in parallel with $C_{\rm soc}$. However, this paper omits the battery's self-discharge as it involves a relatively large time constant.

B. UESM: Supercapacitor

Numerous supercapacitor equivalent circuit models exist in literature with various topologies. An in-depth discussion on each modeling approach is out of the scope of this paper, but readers can refer to [14], [18] for review and comparisons. In general, supercapacitor equivalent circuit models are grouped in RC parallel branch dynamic models, multi-stage RC ladder (or transmission line) models, and multi-branch RC series models, or a combination of them found in [17]. Aside from the multi-branch RC series model with an incompatible circuit topology, any of these model types is compatible with the UESM. The RC parallel branch dynamic model [14] uses a similar topology as the dynamic battery model used in Section IV-A, thus is not discussed further in this paper.

The remainder of this section will demonstrate how the supercapacitor model presented in [17] can be transformed into the UESM framework. The model is shown in Fig. 6 for the reader's convenience. However, the parallel leakage (self-discharge) resistor R_p is moved to the left side of the series resistor R_s , and into the SOC domain, to fit the UESM. Given the resistance magnitude difference between R_p and R_s , this minor change in model topology results in a negligible error.

The dotted line in Fig. 6 marks the separation between the SOC and electrical domain. The resulting UESM representation is shown in Fig. 7. All circuit elements in the electrical domain are identical to the corresponding elements from [17]. The SOC domain circuit elements are derived by transforming the circuit

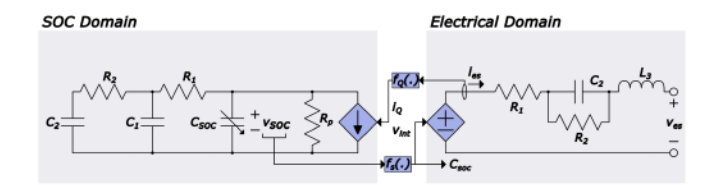


Fig. 7. Supercapacitor UESM.

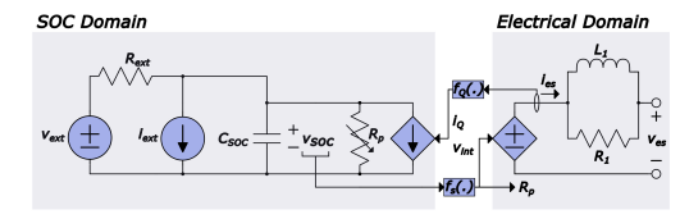


Fig. 8. HVAC UESM.

elements shown on the left side of Fig. 6 using (6)–(7). Similar to the battery UESM, the SOC domain discharge current i_Q is equivalent to the supercapacitor's output current i_{es} . The relation between $v_{\rm soc}$ of the SOC domain and v_{int} of the electrical domain is $v_{int} = V_{\rm max} v_{\rm soc}$ where $V_{\rm max}$ is the rated voltage of the supercapacitor.

C. UESM: HVAC-Based Virtual Energy Storage

For an HVAC-based VES, energy is stored using the thermal capacitance of the building's air. Therefore, the SOC domain models the building's thermodynamics, where the SOC is proportional to the temperature T_b . Feeding power into the VES (i.e., cooling the building) results in the charging of the ES. Since the HVAC system in this scenario provides only cooling to the building, an SOC = 1 occurs at its minimum temperature limit ($T_b = T_{\min}$) and SOC = 0 at its maximum ($T_b = T_{\max}$). The thermodynamic parameters of (4) are scaled using (5)–(7), with $x_0 = T_{\text{max}}$, $x_1 = T_{\text{min}}$. This VES has both an external voltage source v_{ext} and current source i_{ext} . v_{ext} is equivalent to T_{amb} scaled using (5), while i_{ext} is Q_o of (4) and not scaled. The original system (Fig. 2) models the HVAC cooling as a Thevenin source with constant temperature T_l and variable thermal resistance R_{hvac} . To match the UESM framework, this Thevenin source is converted into the Norton equivalent where R_{hvac} is converted into R_p using (7). The SOC domain circuit for this VES is shown in Fig. 8.

The electrical domain for real energy storage consists of an SOC-dependent voltage source and series impedance intrinsic to the storage physics. The series impedance, in turn, defines the transient response of the output voltage v_{es} for a change in load current. For this VES, the transient response of v_{es} primarily depends on the implemented control system. As discussed in Section II, temperature regulation and power filtering is controlled by the dc/dc converter while the motor drive regulates the dc-link capacitor voltage. The electrical domain circuit should then represent the behavior of the voltage PI controller, which outputs a command current i based on the error between referenced and measured voltage ($e = v^* - v$). This is analogous to a

current through an impedance between two voltage sources (i.e., $e=i\cdot Z$ where $Z^{-1}=PI(s)$). The voltage controller circuit representation uses methods derived in [40], [41]. The electrical domain for this VES thus consists of a voltage source with a magnitude of the reference dc-link voltage and a parallel RL impedance. R represents the inverse proportional gain and L represents the inverse integral gain. This circuit representation is shown in Fig. 8. In the case that the voltage controller parameters do not change, the UESM component-states function outputs constant values independent to the SOC.

The UESM discharge function handles the conversion between the electrical domain i_{es} and SOC domain i_Q . For HVAC-based VES, i_Q is the heat transfer induced by the cooling system. From (4), $i_Q = -c_p \dot{m} T_l$, where \dot{m} is a function of w_{fan} given in (1) and is indirectly controlled by i_{es} . A steady-state equation for i_{es} as a function of the fan speed w_{fan} is derived below.

This work considers an HVAC system that uses a PMSM, but other machine types can be used and requires deriving a new discharge function to match the machine type. Detailed modeling of machine dynamics, including reluctance and cogging torque, is not the emphasis of this work as they provide little benefit when considering the HVAC energy system. Therefore, the widely used machine electrical and mechanical dynamics are used, covered in textbooks such as [42].

The rotational dynamics of a cylindrical PMSM driving a fan operating with no flux weakening (i.e., $i_{sd} = 0$) is modeled as

$$J\frac{d}{dt}w_{fan} = \frac{p}{2}\lambda_m i_{sq} - k_2 w_{fan}^2 - Bw_{fan}$$
 (14)

where J is the combined motor and fan rotational inertia, λ_m is the PMSM flux linkage, i_{sq} is the q-axis current, and B is the frictional loss coefficient of the motor [42]. Combining the power-invarient rotating reference dq-frame active power equation $P = v_{sq}i_{sq}$ (reduced from $P = v_{sd}i_{sd} + v_{sq}i_{sq}$ since $i_{sd} = 0$), inverter input power $P = i_{es}v_{dc}$ and the steady-state q-axis equivalent circuit voltage formula (15) yields the relation (16)

$$v_{sq} = \frac{p}{2} \lambda_m w_{fan} + R_s i_{sq} \tag{15}$$

$$R_s i_{sq}^2 + \frac{p}{2} \lambda_m w_{fan} i_{sq} = i_{es} v_{dc}$$
 (16)

where R_s is the stator resistance, p is the PMSM pole count, and v_{dc} is the dc input voltage of the inverter. Solving (16) for i_{sq} results in the quadratic equation

$$i_{sq} = \frac{-\frac{p}{2}\lambda_m w_{fan} + \sqrt{(\frac{p}{2}\lambda_m w_{fan})^2 + 4R_s i_{es} v_{dc}}}{2R_s}$$
(17)

Inserting (17) into (14) under steady-state conditions ($\frac{d}{dt}w_{fan}=0$) and solving for i_{es} results in a quartic equation dependent on only two time-varying components, w_{fan} and v_{dc} , where w_{fan} is present to the fourth order. For the VES UESM discharge function, v_{dc} is assumed to be constant, thus the quartic equation for i_{es} is solely dependent on w_{fan} , or $i_{es}=f(w_{fan})$. Due to the size of the quartic equation, it is omitted from this paper. Solving for i_Q as a function of i_{es} requires the inverse solution to the quartic equation. Since solving such an equation is a

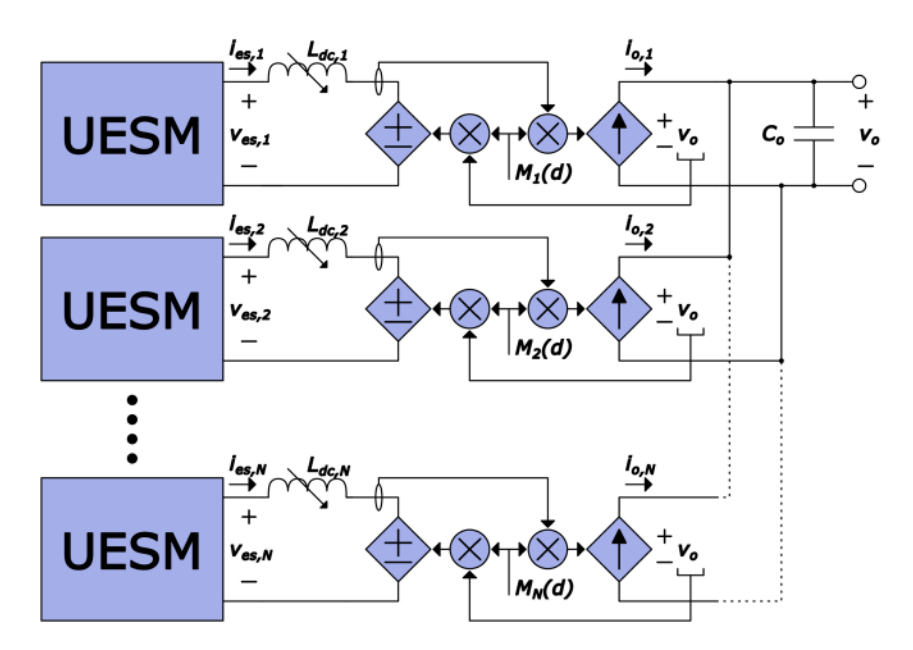


Fig. 9. The UHESM generic diagram. The number of UESM and power converter instances depend on the amount of energy storage devices of the HESS.

time-intensive procedure, an inverse-function lookup table is generated by evaluating $i_{es}=f(w_{fan})$ for a range of w_{fan} values between 0 and the fan's rated speed. This lookup table serves as the UESM discharge function.

V. UNIVERSAL HYBRID ENERGY STORAGE MODEL

This section proposes a design-oriented universal hybrid energy storage model (UHESM) that captures the characteristics and dynamics of a dc-connected hybrid storage system. A hybrid storage system consists of multiple energy storage types either connected via power electronics or their terminals directly. It should be emphasized that this work considers only hybrid storage systems interfaced with dc/dc converters. Since the majority of storage devices utilize a dc connection, this constraint does not inhibit the universality of the UHESM. Even storage devices with "ac" storage such as flywheels or pumped hydro require a dc-interface to convert their variable frequencies to a regulated frequency in the scenario of an ac-interfaced system (e.g., ac/dc/ac conversion between storage and the grid) [24]. A dc-interfaced system, focused on in this work, at a minimum only requires the rectification of the "ac" storage device to a dc-link (e.g., ac/dc conversion between storage and distribution bus). Modeling the ac/dc converter stage is compatible with the UHESM, as was demonstrated for the VES in Section IV-C where the ac/dc converter driving the HVAC motor is lumped into the UESM.

There are a variety of hybrid storage topologies that exist to represent these connection options, such as passive, active, and semi-active [37], [38]. There are also a wide variety of dc/dc power converter types to choose from. However, regardless of converter type or system topology, a delay in energy transfer between the storage and load is introduced via converter impedance and the control system. These characteristics influence the response time and transients, i.e., the feasible bandwidth's upper frequency limit that the storage can filter and its stability.

The dynamic commonalities among architectures are leveraged in the UHESM. Not only is it able to model a wide variety of systems, it also aims to simplify early design stages through generalization. While the system topology and converter types impact dynamic characteristics, it is shown through the UHESM that a crucial design stage can precede those decisions. Rather than considering converter and topology details and analyzing their impacts on bandwidth and stability, the UHESM facilitates the approach of selecting energy storage types, architecture requirements, and controls based on the required bandwidths. Once this information is known, the generalized parameters can be transformed to explore optimal converter types and topology options.

The UHESM, shown in Fig. 9, is capable of representing a wide variety of HESS regardless of the topology and power electronic dc/dc converters being used. It consists of an arbitrary number of parallel-connected energy storages optionally interfaced through power electronic converters. This is an extension of the UESM presented in Section III, which can model any type of energy storage device itself but does not include power electronics or topological configurations required for a hybrid storage system. The UHESM aggregates multiple instances of the UESM into a single model using a generalized converter/system framework. The connection between each energy storage and the systems output is modeled as a generalized converter interface; however, it is shown how it can behave as if no converter was used (such as in a passive topology). This development is discussed in Section V-A. While the UHESM structure appears to match the active topology, it is actually compatible with any of the HESS topologies, further explored in Section V-B.

A. Generalized DC/DC Power Electronic Converter Model

The converter interface in the UHESM is shown in Fig. 10 with a conventional current controller feedback loop. Converter modeling utilizes the switching averaging technique, which

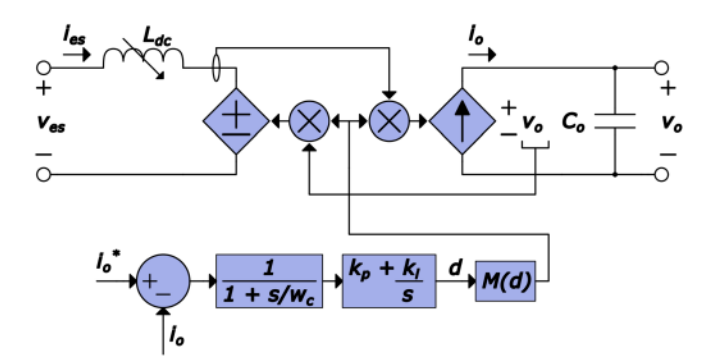


Fig. 10. Generalized dc/dc converter switching averaged model.

TABLE I CONVERTER PARAMETERS

Converter	L	M(d)
Buck	$\frac{L'}{Nd^2}$, for N interleaved converters	$\frac{1}{d}$
Boost	$\frac{L'}{N}$, for N interleaved converters	1-d
Buck-boost	$\frac{L'}{Nd^2}$, for N interleaved converters	$\frac{1-d}{d}$
No converter	0	1

transforms a switch module into dependent voltage and current sources by averaging the multiple circuit states together [43]. The behavior of the two dependent sources is akin to a traditional AC transformer, where the winding turns ratio is replaced by the converter's duty cycle. Thus, it is often referred to as a "dc transformer". This generalized converter model is primarily based on the canonical model from [43], which includes how the buck, boost, and buck-boost converters can be represented as the same circuit with varying parameters. However, in [43], the canonical model is linearized for small-signal analysis, whereas Fig. 10 is nonlinear and for large-signal analysis. Additionally, the canonical model has the inductor on the right side of the "dc transformer", whereas Fig. 10 has the inductor on the left side. The inductor placement is different for conceptual reasons and does not impact model behavior. The controller consists of a low-pass filter to remove measured switching dynamics and a PID function. Once properly tuned, it will closely follow the reference output current i^* by adjusting the duty cycle d. How d impacts the converter is topology-dependent and is contained in the modulation function M(d).

In addition to the basic converters, this generalized dynamic model can also represent interleaved converters and no converter. Each possible converter is shown in Fig. 11 for readers' comprehension, and their specific parameters are given in Table I. Only a circuit diagram for an interleaved boost converter is shown, but any of the other dc/dc converters can be interleaved in the same manner. The control system is shared among the interleaved converters, where the measured output current i_o in Fig. 10 is the combined current of all N converters. Likewise, controller output d is identical for each converter. For non-interleaved converters, simply use N=1 for the parameters in Table I. The input and output capacitors are shared for the interleaved converters and are thus impacted by N.

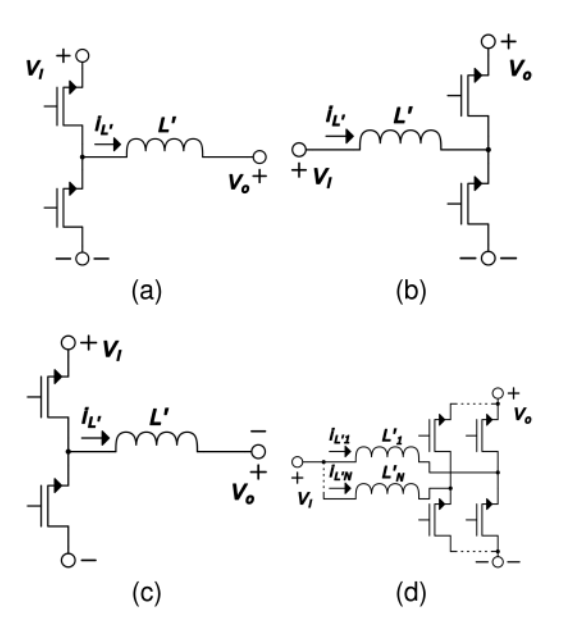


Fig. 11. Various dc/dc converter topologies that the UHESM can represent. (a) buck, (b) boost, (c) buck-boost, (d) interleaved boost converters.

The state-space (18)–(19) are used to model the generalized dc/dc converter. Equation notation is for the UHESM of Fig. 9. One circuit element states exist for each storage converter instance n: the converter input current $i_{l,n}$, dependent on the converter inductance $L_{dc,n}$. The change in $i_{l,n}$ is determined by (18). A single output capacitor is shared among all storages of the HESS, C_o , and its voltage state is calculated using (19). Some UESM instances may include a series inductance, such as the presented supercapacitor Fig. 7. To avoid any KCL violations, the UESM series inductance is added to $L_{dc,n}$, and a single-state equation is used.

$$L_{dc,n} \frac{d}{dt} i_{l,n} = v_{es,n} - v_o M_n(d)$$
 (18)

$$C_o \frac{d}{dt} v_o = \sum_{n=1}^{N} i_{o,n} - i_{load}$$
 (19)

B. UHESM Topology Agnosticism

The different hybrid storage system topologies that the UH-ESM is capable of modeling are shown in Fig. 12. Each configuration and the UHESM parameter relations are discussed below.

- 1) Active: The UHESM is equivalent to the active topology when the circuit parameters and controls of each converter are independent. For a two-storage active configuration, shown in Fig. 12(a), these UHESM relations apply: $M_1(d) \neq M_2(d)$, $L_1 \neq L_2$, $C_1 \neq C_2$.
- 2) Semi-Active: The UHESM is equivalent to the semi-active topology when one converter is nulled using the parameters given in Table I. For a two-storage active configuration, shown in Fig. 12(b), these UHESM relations apply: $M_1(d) \neq M_2(d) = 0$, $L_1 \neq L_2 = 0$, $C_1 \neq C_2 = 0$.

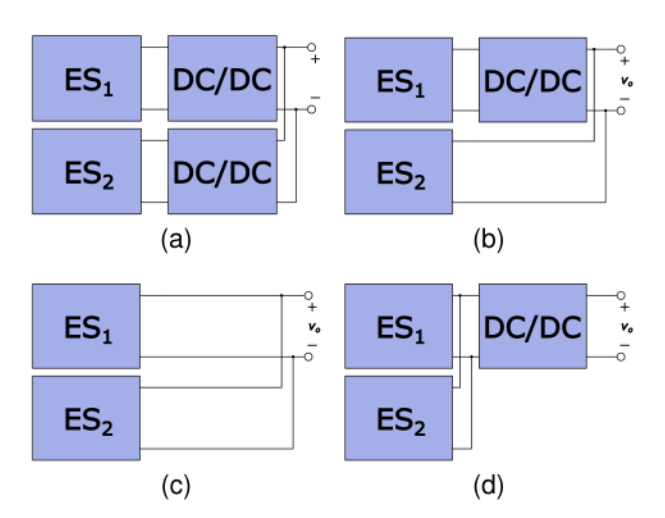


Fig. 12. The HESS topologies that the UHESM can represent. The configurations shown are (a) active, (b) semi-active, (c) passive without power electronics, (d) passive with power electronics.

- 3) Passive Without a Converter: The UHESM is equivalent to the passive topology without power converters when all converters are nulled using the parameters given in Table I. For a two-storage passive configuration without converters, shown in Fig. 12(c), these UHESM relations apply: $M_1(d) = M_2(d) = 0$, $L_1 = L_2 = 0$, $C_1 = C_2 = 0$.
- 4) Passive With a Converter: The UHESM is equivalent to the passive topology with power converters when the circuit parameters and controls of each converter are shared. For a two-storage passive configuration with converters, shown in Fig. 12(d), these UHESM relations apply: $M_1(d) = M_2(d)$, $L_1 = L_2$, $C_1 = C_2$, and $i_o = i_{o,1} + i_{o,2}$ where i_o is fed into the current controller.

VI. UHESM DEMONSTRATION AND VALIDATION

Typical switching models are fully validated with hardware in many literature and are trustworthy. This section validates the proposed UHESM (Fig. 9) and the UESM (Fig. 4) emphasizing the HVAC VES by comparing it to an equivalent switching model discussed in Section II, while integrated battery, supercapacitor, and power electronics are also included. While the battery and supercapacitor UESM implementations are very similar to the adapted equivalent circuit models, a comparison of the battery and supercapacitor UESM's is included for completeness. An overview of the system and simulation used to demonstrate the UHESM is given first. All models and comparisons for this paper are built and performed using PLECS software.

A. Simulation Overview

The hybrid energy storage system used to demonstrate the UHESM consists of three energy storage devices: battery, supercapacitor, and HVAC VES. Each of them is modeled using the UESM of Section III and connected together via power electronics. The parameters used in the simulations for a Li-ion battery, supercapacitor, and HVAC VES come from [5], [17], and [2], respectively. The battery module is a single cell, and the

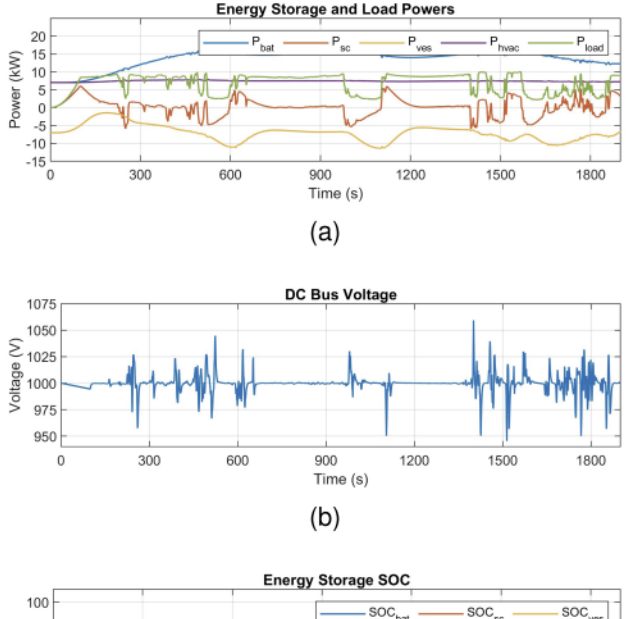
TABLE II Hybrid Energy Storage System Model Parameters

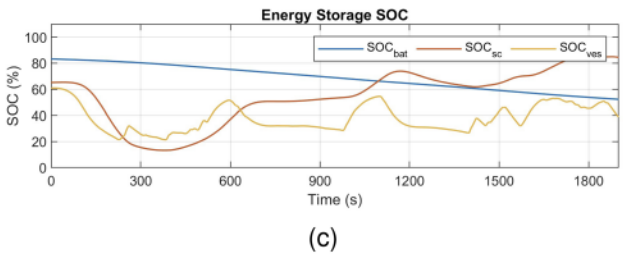
Device	Model parameters	
Battery	$C_{SOC} = 7920\mathrm{F}$	
(SOC Domain)		
Battery	$N_s = 474, N_p = 6$	
(Electrical Domain)		
Supercapacitor	$C_{SOC,0} = 3348 \mathrm{F},$	
(SOC Domain)	$C_{SOC,1} = 585.9 \mathrm{F}, R_p = 3.52 \mathrm{k}\Omega,$	
	$R_1 = 0.1085 \Omega$, $C_1 = 428.2 \mathrm{F}$,	
	$R_2 = 7.750 \Omega, C_2 = 464.6 \mathrm{F}$	
Supercapacitor	$N_s = 18, N_p = 1, R_1 = 6.625 \mathrm{m}\Omega,$	
(Electrical Domain)	$R_2 = 2.4 \mathrm{m}\Omega, C_2 = 28.4 \mathrm{F},$	
	$L_{es}=404\mathrm{nH}$	
HVAC VES	$C_{SOC}=1.4\mathrm{MF},R_{ext}=2.5\mathrm{m}\Omega$	
(SOC Domain)	$v_{ext} = -4.5 \mathrm{V}, i_{ext} = 11.5 \mathrm{kA}$	
HVAC VES	$R_1 = 2 \Omega, L_1 = 10 \mathrm{H},$	
(Electrical Domain)	$L_{es}=1\mathrm{mH}$	
Buck	N = 1, L' = 1 mH,	
	$f_{sw}=10\mathrm{kHz}$	
Interleaved Boost	$N = 2, L' = 10 \mathrm{mH},$	
	$f_{sw}=10\mathrm{kHz}$	
Buck-boost	$N = 1, L' = 10 \mathrm{mH},$	
	$f_{sw}=10\mathrm{kHz}$	
dc-bus capacitor	$C=100\mu\mathrm{F}$	
Voltage Regulator	$k_p = 0.0628, k_i = 0.03$	
Filters	$G_{0,1}=1,\omega_1=2\pi\cdot 1.1{ m mrad/s},$	
	$G_{0,2} = 0.5, \omega_2 = 2\pi \cdot 5 \text{mrad/s}$	
Current Controller	$\omega_c = 2\pi \cdot 2.5 \text{krad/s}, k_p = 0.013, k_i = 15.791$	

supercapacitor module has 18 cells in series. For each storage device, modules are connected in parallel and stacked in series to achieve the desired voltage and capacities. The original HVAC system in [5] is scaled down to match the PMSM power rating of 15 kW and building's volume and heat gain are scaled proportionally to maintain the same rate of heat gain when the HVAC is off. The building's external temperature T_{ext} and heat gain Q_0 are for peak temperatures of a hot summer day, thus providing a conservative scenario for the presented ES metrics. Table II provides the system parameters necessary for the simulations and validation. Battery electrical-domain circuit elements are omitted from Table II but can be found in [5].

To demonstrate the capability of the UHESM to model different dc/dc converters, the battery is interfaced with the dc bus through a buck converter (Fig. 11(a)), the supercapacitor through two interleaved boost converters (Fig. 11(d)), and the HVAC VES through a buck-boost converter (Fig. 11(c)). This results in a hybrid storage active topology, visualized in Fig. 12(a). Each converter utilizes the same current controller shown in Fig. 10 with parameters given in Table II.

Second-order Butterworth low-pass filters $F_n(s)$ (20) are used to split the reference current output of the dc bus voltage regulator among the three energy storage devices. The battery handles the low-frequency component of the load, with filter denoted as $F_{bat}(s) = F_1(s)$ with corner frequency ω_1 and dc gain $G_{0,1}$. Due to the limited storage capacity of the HVAC VES, only a portion of the middle frequencies are supplied by the VES. Its filter is given as $F_{ves}(s) = (1 - F_1(s))F_2(s)$ with corner frequency ω_2 and dc gain $G_{0,2}$. The remaining middle frequencies and high frequencies are handled by the supercapacitor, with filter $F_{sc}(s) = 1 - F_1(s) - F_2(s)$. The voltage regulator





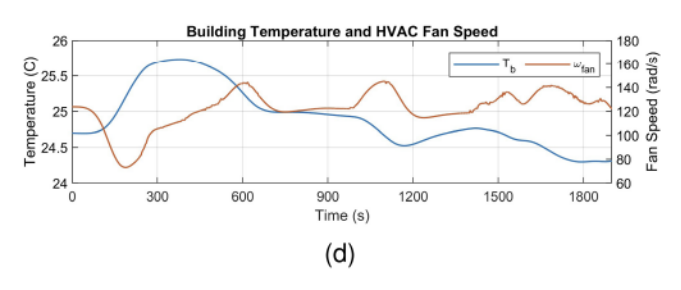
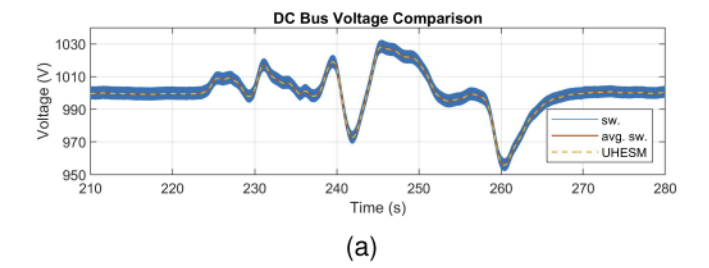


Fig. 13. UHESM model waveforms from simulation. The power profiles of the system load and each energy storage device is given in (a), the dc bus voltage in (b), the SOC of each storage device in (c), and building temperature and HVAC fan speed in (d).

and filter parameters are given in Table II.

$$F_n(s) = \frac{G_{0,n}}{(s/\omega_n)^2 + \sqrt{2}(s/\omega_n) + 1}$$
 (20)

The UHESM is demonstrated through a 30-minute simulation using a load profile based on solar PV power generation. As this hybrid system and load profile is just for demonstration, the parameters and load profile are not meant to be representative of an optimized, real system. The load profile is provided in Fig. 13(a) along with the power waveforms for each energy storage device. Note that HVAC power profile is always negative as the HVAC is a unidirectional load in practice. However, it effectively serves in a bidirectional manner for a given bandwidth due to the constant dc-load also shown in Fig. 13(a). In addition to maintaining nominal temperatures using the HVAC, the HESS regulates the dc bus voltage connected to the load. Fig. 13(b) shows the dc bus voltage throughout the simulation. The SOC of



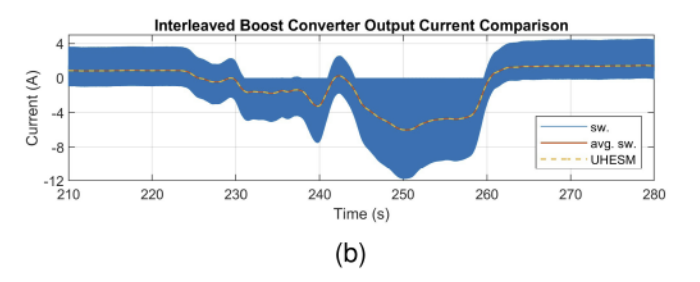


Fig. 14. Comparison between the switching-averaged model waveforms of the UHESM and a switching simulation.

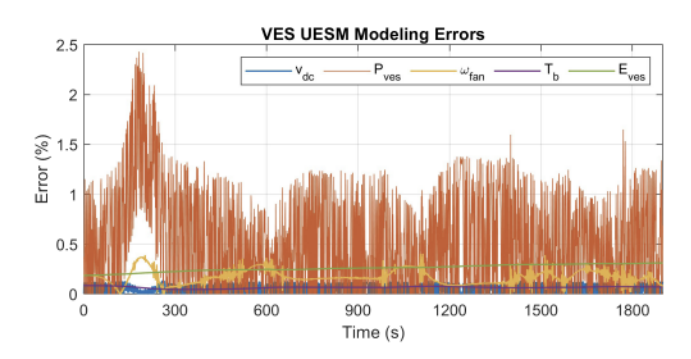
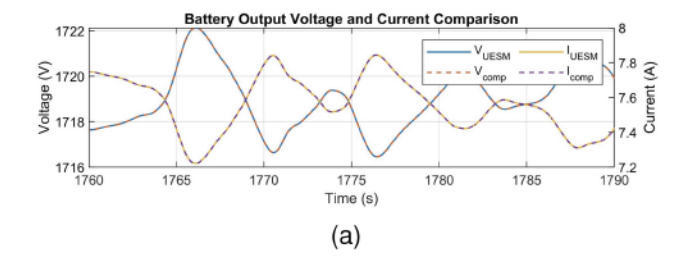


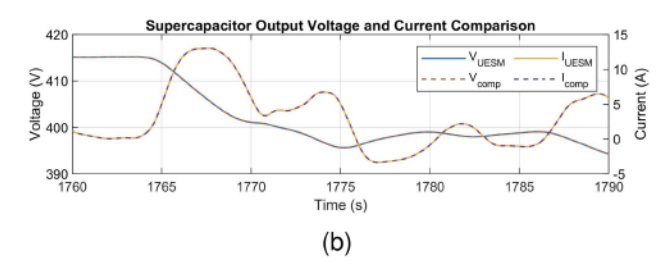
Fig. 15. UESM modeling errors for HVAC VES compared to switching model.

each energy storage device throughout the simulation is plotted in Fig. 13(c). While the SOC of the HVAC VES is directly proportional to the building's temperature T_b , it is provided in Fig. 13(d) accompanied by the HVAC fan speed ω_{fan} .

B. UHESM and Switching Model Comparison

The UHESM utilizes switching-averaged modeling for the dc/dc converters. As this approach is widely used in literature and validated, only a brief comparison between the UHESM and a switching model is given. As the name implies, the switching states of the converters are averaged to create continuous voltage and current waveforms. This removes the switching ripples inherent to a power electronic converter. However, the averaged model preserves most other transients with frequencies lower than the switching frequency. This can be observed in Fig. 16, which compares the UHESM (Fig. 9) and switching models simulated dc bus voltage v_o and the output current of the interleaved boost converter $i_{o,3}$ connected to a supercapacitor. In Fig. 14(a), it is shown the equality of v_o of the switching simulation's periodic average compared to that of the UHESM. A similar equality is observed in Fig. 14(b) for $i_{o,3}$. This demonstrates that





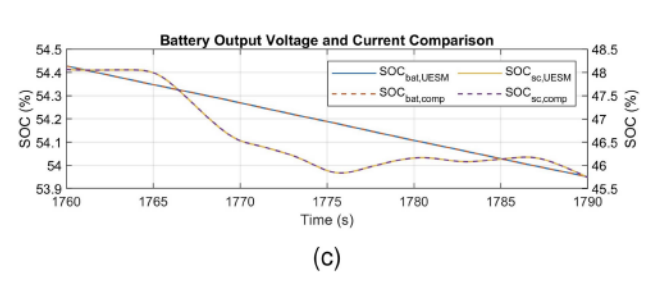


Fig. 16. Simulation plots comparing the UESM and original equivalent circuit models for the battery and supercapacitor. (a) Compares the output voltage and current of both models for the battery. (b) Compares the output voltage and current of both models for the supercapacitor. (c) Compares the SOC of both models for both battery and supercapacitor.

while converter switching transients are a vital consideration in converter design, they have little impact on the system dynamics.

The advantage of the UHESM over switching models is similar to conventional switching-averaged dynamic models. Simulating the equivalent switching model of this system involves multiple switching states per converter, with a simulation period T_{sim} sufficiently small to capture switching dynamics (i.e., $T_{sim} \ll f_{sw}^{-1}$). Simulations at this granularity become unreasonable for long-duration studies (such as the 30-min demonstration of Fig. 13), especially when integrated within a design process that involves many simulation iterations. The computational complexity only increases with switching frequency or the number of converters used in the system. While conventional dynamic models avoid the increased complexity from switching frequency, the UHESM also avoids increased complexity caused by the number of converters in the system. Combining N interleaved converter circuit and control states into a single dynamic converter model requires less computation. Additionally, any change in the architecture is achieved by simply adjusting the UHESM input parameters rather than modifying the simulation model.

C. HVAC-Based VES UESM Model Validation

The VES UESM shown in Fig. 8 connects to the switching averaged-equivalent dc/dc converter of the switching model

shown in Fig. 2. The SOC domain circuit is mathematically equivalent to the thermal circuit in the switching model and thus behaves identically. The primary difference between the two models is the implementation of the inverter and motor. The UESM abstracts away the inverter by using a circuit representation of the voltage PI controller realized by the inverter, while the motor is part of the UESM discharge function $f_Q(\cdot)$. This approach means that within the UESM there is no direct feedback between the motor and the dc-link voltage regulator nor electrical or mechanical transients. While this does introduce a modeling error, the impact is minimal. Additionally, no dc-link capacitor is modeled in the UHESM. As this capacitor's primary purpose is to filter switching ripples, it is not necessary in the dynamic model.

Fig. 15 compares the VES waveforms of the UESM and switching model from a 30-min simulation. The VES filters the power signal P_{load} shown in Fig. 13(a). The largest error between models appears in the output power P_{ves} , with a max absolute error (MAE) of 2.43%. However, the power error does not accumulate as fast, as the energy E_{ves} MAE throughout the simulation is only 0.31%. The MAE error for v_{dc} , ω_{fan} , and T_b are 0.14%, 0.40%, and 0.08%, respectively. These results demonstrate that the UESM can simulate the behavior of the HVAC-based VES to a high degree of accuracy, with the benefit of running much faster.

D. Battery and Supercapacitor UESM Model Comparisons

The same simulation scenario discussed in Section VI-A is repeated but with the original battery and supercapacitor equivalent circuit models from [5] and [17] that the UESM models adapt from. Results from this new simulation validate the battery and supercapacitor UESM.

The only difference between the battery UESM (Fig. 5) and the equivalent circuit model in [5] is the scaling of the SOC domain circuit components. The scaling in the UESM normalizes the SOC domain's voltage so that $v_{\rm soc}$ represents the SOC of the storage device. However, this normalization does not mathematically alter the behavior of the model. Therefore, the battery UESM behaves identically to the model in [5]. This is demonstrated in Fig. 16(a), comparing the output voltage and current of the two models, which correspond to a snapshot of the simulation results of Fig. 13. From Fig. 16(a), there is a perfect overlap between the signals of the two models. Fig. 16(c) shows that the SOC of both battery models also matches.

Unlike the battery UESM adaptation of [5], the supercapacitor UESM (Fig. 7) requires some alteration of the equivalent circuit model in [17] (Fig. 6), as was discussed in Section IV-B. In addition to the circuit component scaling for the SOC domain, R_p in Fig. 6 is also moved to be in parallel with $C_{\rm soc}$. While this changes the equivalent circuit topology, the UESM accuracy is negligibly impacted. This is observed in Fig. 16(b) for the supercapacitor's output voltage and current and Fig. 16(c) for the SOC. The reason for no difference between the two models is mainly due to the magnitude of R_p compared to R_s in Fig. 6. If R_p were a smaller value, resulting in a faster self-discharge of the supercapacitor, more error would occur. Additionally, the value

of R_p from [17] was identified for the specific circuit topology. It is safe to assume that if the supercapacitor UESM parameters were directly identified from application data, any possible error from the circuit topology and location of R_p in the UESM would be mitigated.

VII. CONCLUSION AND FUTURE WORK

A universal hybrid energy storage model is proposed in this paper that is capable of modeling many types of real and virtual energy storage connected via power electronics. The UHESM consists of a universal representation of energy storage devices, utilizing common elements of energy storage equivalent circuit models and separating storage mechanics from electrical dynamics, in addition to a generalized dc/dc converter model. Design exploration and analysis simplifies with the unified modeling theory for power electronic connected energy storages, where design modification simply requires a change in input parameters to the UHESM rather than simulation model development. The modeling theory for both storage and power converters is covered. It is shown how the proposed model is compatible with HVAC-based virtual energy storage and validates its performance by comparing it to a switching model. Further, the UHESM's ability to model various interleaved dc/dc converters is compared to switching models.

Future work will explore how the UHESM framework can aid in designing and analyzing hybrid energy storage systems. Given the modularity and generalization of the framework, it is expected to be compatible with a top-down design methodology that begins with system specifications and sequentially selects optimal system architecture, energy storage types, converter requirements, hybrid system controls, and other design details.

REFERENCES

- D. Jackson and Y. Cao, "A universal modeling framework for real and virtual energy storage," in *Proc. IEEE Energy Convers. Congr. Expo.*, 2023, pp. 208–215.
- [2] Y. Cao, J. A. Magerko, T. Navidi, and P. T. Krein, "Power electronics implementation of dynamic thermal inertia to offset stochastic solar resources in low-energy buildings," *IEEE Trans. Emerg. Sel. Topics Power Electron.*, vol. 4, no. 4, pp. 1430–1441, Dec. 2016.
- [3] H. Hao, T. Middelkoop, P. Barooah, and S. Meyn, "How demand response from commercial buildings will provide the regulation needs of the grid," in *Proc. Annu. Allerton Conf. Commun.*, Control, Comput., 2012, pp. 1908–1913.
- [4] H. Gong, V. Rallabandi, D. M. Ionel, D. Colliver, S. Duerr, and C. Ababei, "Dynamic modeling and optimal design for net zero energy houses including hybrid electric and thermal energy storage," *IEEE Trans. Ind. Appl.*, vol. 56, no. 4, pp. 4102–4113, Jul./Aug. 2020.
- [5] Y. Cao, R. C. Kroeze, and P. T. Krein, "Multi-timescale parametric electrical battery model for use in dynamic electric vehicle simulations," *IEEE Trans. Transp. Electrific.*, vol. 2, no. 4, pp. 432–442, Dec. 2016.
- [6] S. Tamilselvi et al., "A review on battery modelling techniques," Sustainability, vol. 13, no. 18, pp. 1–26, 2021.
- [7] A. Seaman, T.-S. Dao, and J. McPhee, "A survey of mathematics-based equivalent-circuit and electrochemical battery models for hybrid and electric vehicle simulation," *J. Power Sources*, vol. 256, pp. 410–423, 2014.
- [8] X. Hu, S. Li, and H. Peng, "A comparative study of equivalent circuit models for Li-ion batteries," J. Power Sources, vol. 198, pp. 359–367, 2012.
- [9] G. Marin-Garcia, G. Vazquez-Guzman, J. Sosa, A. R. Lopez, P. Martinez-Rodriguez, and D. Langarica, "Battery types and electrical models: A review," in *Proc. IEEE Int. Autumn Meeting Power, Electron., Comput.*, 2020, vol. 4, pp. 1–6.

- [10] S. Tamilselvi, N. Karuppiah, and S. Muthubalaji, "Design of an efficient battery model using evolutionary algorithms," *Periodicals Eng. Natural* Sci., vol. 6, no. 2, pp. 265–282, 2018.
- [11] M. Chen and G. Rincon-Mora, "Accurate electrical battery model capable of predicting runtime and I-V performance," *IEEE Trans. Energy Convers.*, vol. 21, no. 2, pp. 504–511, Jun. 2006.
- [12] C. Zhao, H. Yin, Z. Yang, and C. Ma, "Equivalent series resistance-based energy loss analysis of a battery semiactive hybrid energy storage system," *IEEE Trans. Energy Convers.*, vol. 30, no. 3, pp. 1081–1091, Sep. 2015.
- [13] R. Faranda, "A new parameters identification procedure for simplified double layer capacitor two-branch model," *Electric Power Syst. Res.*, vol. 80, no. 4, pp. 363–371, 2010.
- [14] L. Zhang, Z. Wang, X. Hu, F. Sun, and D. G. Dorrell, "A comparative study of equivalent circuit models of ultracapacitors for electric vehicles," *J. Power Sources*, vol. 274, pp. 899–906, 2015.
- [15] R. Nelms, D. Cahela, and B. Tatarchuk, "Modeling double-layer capacitor behavior using ladder circuits," *IEEE Trans. Aerosp. Electron. Syst.*, vol. 39, no. 2, pp. 430–438, Apr. 2003.
- [16] L. Zhang, X. Hu, Z. Wang, F. Sun, and D. G. Dorrell, "A review of supercapacitor modeling, estimation, and applications: A control/management perspective," *Renewable Sustain. Energy Rev.*, vol. 81, pp. 1868–1878, Jan. 2018.
- [17] A. Berrueta, I. San Martín, A. Hernández, A. Ursúa, and P. Sanchis, "Electro-thermal modelling of a supercapacitor and experimental validation," J. Power Sources, vol. 259, pp. 154–165, 2014.
- [18] F. Naseri, S. Karimi, E. Farjah, and E. Schaltz, "Supercapacitor management system: A comprehensive review of modeling, estimation, balancing, and protection techniques," *Renewable Sustain. Energy Rev.*, vol. 155, pp. 1–19, 2022.
- [19] S. N. M., O. Tremblay, and L.-A. Dessaint, "A generic fuel cell model for the simulation of fuel cell vehicles," in *Proc. IEEE Veh. Power, Propulsion Conf.*, 2009, pp. 1722–1729.
- [20] T. Lan and K. Strunz, "Multiphysics transients modeling of solid oxide fuel cells: Methodology of circuit equivalents and use in EMTP-type power system simulation," *IEEE Trans. Energy Convers.*, vol. 32, no. 4, pp. 1309–1321, Dec. 2017.
- [21] A. M. Dhirde, N. V. Dale, H. Salehfar, M. D. Mann, and T.-H. Han, "Equivalent electric circuit modeling and performance analysis of a PEM fuel cell stack using impedance spectroscopy," *IEEE Trans. Energy Convers.*, vol. 25, no. 3, pp. 778–786, Sep. 2010.
- [22] X. Luo, J. Wang, M. Dooner, and J. Clarke, "Overview of current development in electrical energy storage technologies and the application potential in power system operation," *Appl. Energy*, vol. 137, pp. 511–536, Jan. 2015.
- [23] R. Georgious, R. Refaat, J. Garcia, and A. A. Daoud, "Review on energy storage systems in microgrids," *Electronics*, vol. 10, no. 17, 2021, Art. no. 2134.
- [24] J. Mitali, S. Dhinakaran, and A. A. Mohamad, "Energy storage systems: A review," *Energy Storage Saving*, vol. 1, no. 3, pp. 166–216, 2022.
- [25] H. A. Behabtu et al., "A review of energy storage technologies' application potentials in renewable energy sources grid integration," *Sustainability*, vol. 12, no. 24, pp. 1–20, 2020.
- [26] E. Severson, R. Nilssen, T. Undeland, and N. Mohan, "Magnetic equivalent circuit modeling of the AC homopolar machine for flywheel energy storage," *IEEE Trans. Energy Convers.*, vol. 30, no. 4, pp. 1670–1678, Dec. 2015.
- [27] C.-T. Pham and D. Månsson, "On the physical system modelling of energy storages as equivalent circuits with parameter description for variable load demand (Part I)," J. Energy Storage, vol. 13, pp. 73–84, 2017.
- [28] C.-T. Pham and D. Månsson, "Optimal energy storage sizing using equivalent circuit modelling for prosumer applications (Part II)," J. Energy Storage, vol. 18, pp. 1–15, 2018.
- [29] H. Hao, D. Wu, J. Lian, and T. Yang, "Optimal coordination of building loads and energy storage for power grid and end user services," *IEEE Trans. Smart Grid*, vol. 9, no. 5, pp. 4335–4345, Sep. 2018.
- [30] A. Khaligh and Z. Li, "Battery, ultracapacitor, fuel cell, and hybrid energy storage systems for electric, hybrid electric, fuel cell, and plug-in hybrid electric vehicles: State of the art," *IEEE Trans. Veh. Technol.*, vol. 59, no. 6, pp. 2806–2814, Jul. 2010.
- [31] J. Shen and A. Khaligh, "A supervisory energy management control strategy in a battery/ultracapacitor hybrid energy storage system," *IEEE Trans. Transp. Electrific.*, vol. 1, no. 3, pp. 223–231, Oct. 2015.
- [32] R. Carter, A. Cruden, and P. J. Hall, "Optimizing for efficiency or battery life in a battery/supercapacitor electric vehicle," *IEEE Trans. Veh. Technol.*, vol. 61, no. 4, pp. 1526–1533, May 2012.

- [33] M.-E. Choi, J.-S. Lee, and S.-W. Seo, "Real-time optimization for power management systems of a battery/supercapacitor hybrid energy storage system in electric vehicles," *IEEE Trans. Veh. Technol.*, vol. 63, no. 8, pp. 3600–3611, Oct. 2014.
- [34] M. Zarghami, M. L. Crow, J. Sarangapani, Y. Liu, and S. Atcitty, "A novel approach to interarea oscillation damping by unified power flow controllers utilizing ultracapacitors," *IEEE Trans. Power Syst.*, vol. 25, no. 1, pp. 404–412, Feb. 2010.
- [35] Z. Amjadi and S. S. Williamson, "Prototype design and controller implementation for a battery-ultracapacitor hybrid electric vehicle energy storage system," *IEEE Trans. Smart Grid*, vol. 3, no. 1, pp. 332–340, Mar. 2012.
- [36] J. Qin, Y. Chow, J. Yang, and R. Rajagopal, "Distributed online modified greedy algorithm for networked storage operation under uncertainty," *IEEE Trans. Smart Grid*, vol. 7, no. 2, pp. 1106–1118, Mar. 2016.
- [37] T. S. Babu, K. R. Vasudevan, V. K. Ramachandaramurthy, S. B. Sani, S. Chemud, and R. M. Lajim, "A comprehensive review of hybrid energy storage systems: Converter topologies, control strategies and future prospects," *IEEE Access*, vol. 8, pp. 148702–148721, 2020.
- [38] T. Dragičević, X. Lu, J. C. Vasquez, and J. M. Guerrero, "DC microgrids— Part I: A review of control strategies and stabilization techniques," *IEEE Trans. Power Electron.*, vol. 31, no. 7, pp. 4876–4891, Jul. 2016.
- [39] B. Johnson, M. Lu, V. Purba, and S. Dhople, "Circuit-equivalent models for current-controlled inverters," in *Proc. 20th Workshop Control Model. Power Electron.*. Toronto, ON, Canada, 2019, pp. 1–5.
- [40] Q. Zhang et al., "Output impedance modeling and high-frequency impedance shaping method for distributed bidirectional DC-DC converters in DC microgrids," *IEEE Trans. Power Electron.*, vol. 35, no. 7, pp. 7001–7014, Jul. 2020.
- [41] R. Mallik et al., "Equivalent circuit models of voltage-controlled dual active bridge converters," in Proc. 20th Workshop Control Model. Power Electron., 2019, pp. 1–4.
- [42] N. Mohan, Advanced Electric Drives: Analysis, Control, and Modeling Using MATLAB/Simulink. Hoboken, NJ, USA: John Wiley & Sons, 2014.
- [43] R. W. Erickson and D. Maksimović, Fundamentals of Power Electronics, 3rd ed. Cham, Switzerland: Springer, 2020.



Yue Cao (Senior Member, IEEE) received the B.S. degree (with Hons.) in electrical engineering with a second major in mathematics from the University of Tennessee, Knoxville, TN, USA, in 2011, and the M.S. and Ph.D. degrees in electrical engineering from the University of Illinois at Urbana–Champaign (UIUC), Champaign, IL, USA, in 2013 and 2017, respectively. He is currently an Associate Professor with the Energy Systems Group, Oregon State University (OSU), Corvallis, OR, USA. He was a Research Scientist with the Propulsions Team at Ama-

zon Prime Air in Seattle, WA, USA. He was also a Power Electronics Engineer Intern with Special Projects Group, Apple Inc., Cupertino, CA, USA, Halliburton Company, Houston, TX, USA, and Oak Ridge National Laboratory, TN, respectively. His research interests include power electronics, motor drives, and energy storage with applications in renewable energy integration and transportation electrification. Dr. Cao was the recipient of the Myron Zucker Student Award from the IEEE Industry Applications Society (IAS) in 2010, the National Finalist of the USA Mathematical Olympiad (USAMO) in 2006 and 2007, Oregon State Learning Innovation Award for transformative education in 2020, 2022 NSF CAREER Award, got selected into U.S. National Academy of Engineering (NAE) Frontiers of Engineering (FOE) Class of 2022, and the Annual OSU Promising Scholar Award in 2023. He was the Tutorials Chair and Special Sessions Chair of the 2021-2022 IEEE Energy Conversion Congress Expo (ECCE). He is also the Vice Chair of IEEE Power Electronics Society (PELS) TC11 - Aerospace Power. He is an Associate Editor for IEEE TRANSACTIONS ON TRANSPORTATION ELECTRIFICATION, IEEE TRANSACTIONS ON INDUSTRY APPLICATIONS, and IEEE JOURNAL OF EMERGING AND SELECTED TOPICS IN POWER ELECTRONICS.



Derek Jackson (Member, IEEE) received the B.S. and M.S. degrees in electrical and computer engineering and the Ph.D. degree in electrical and computer engineering from Oregon State University (OSU), Corvallis, OR, USA, in 2019, 2021, and 2024, respectively. He was an Engineering Intern with Daimler Trucks NA and Blount International (now Oregon Tool), Portland, OR, and was also a Graduate Researcher with National Renewable Energy Laboratory (NREL). In 2024, he was a Graduate Research Assistant with Energy Systems Group, OSU. He is

currently a Researcher with Electric Vehicle Grid Integration Team, NREL, Golden, CO, USA, where he researches electric vehicle charging solutions, including residential and high-power charging facility system design and controls. His research interests include modeling, optimization, energy storage systems, and motor drives.